

A method is proposed for measuring the detachment distance of the forward shock wave from the surface of a free-flying blunt body. The effect of excitation of vibrational degrees of freedom of the gas on the position of the detached shock wave is investigated for air and carbon dioxide.

The location of the detached shock wave on the axis of flow symmetry is an easily measured flow characteristic that is significantly affected by the excitation of internal degrees of freedom in the gas behind the detached shock [1-3]. By comparing the measurements with theoretical calculations for perfect and equilibrium gas flows, the thermodynamic state of the gas in the shock layer can be successfully determined for the experimental conditions. On the other hand, the experimental data for nonequilibrium flow enable us to check and refine the reaction rate constants [3, 4].

The ballistic method is the most efficient for studying the effect of the real properties of gases on shock detachment. Under the conditions of the ballistic experiment, thermodynamic equilibrium always exists in the incident flow, assuming strictly specified and controlled initial experimental conditions (gas composition, pressure, and temperature), but behind the forward shock wave, depending on the velocity of the model, real gas effects can be reproduced: vibrational excitation, dissociation, and ionization.

In [1, 3] the detachment distance was measured under free flight conditions by photographing the flow spectra using pulsed light sources. Blurring of the flow spectrum, due to the finite exposure time, was compensated by means of a rotating mirror. This method has a number of serious shortcomings. More accurate results over a wide range of model velocities and initial pressures can be obtained using the new

method proposed below. The advantage of this method is the total exclusion of errors associated with the refraction of light rays in the shock layer.

The ballistic apparatus on which the experiments were carried out is shown schematically in Fig. 1. The hemispherical models 15 and 57 mm in diameter, were projected by means of an accelerating device 1. The ballistic tube comprises two sections: an auxiliary chamber 2, and a working chamber 6. In the working chamber, in two mutually perpendicular directions, there are through windows 9, formed by plane-parallel glass plates, through which the flow spectrum and the silhouette of the model are observed. Chambers 2 and 6 are first evacuated to a pressure of 10^{-1} to 5×10^{-2} mm Hg with backing pump 11, after which the working chamber is filled to a specified pressure with the gas under investigation from a cylinder 12. This pressure is registered by a mercury or special oil manometer 4. The end openings of chambers 2 and 6 are closed with thin cellophane membranes, or photographic film. Air leakage into the working chamber was less than 1×10^{-2} mm Hg per minute. In the experiments with carbon dioxide, it was our intent to dry the gas by passing it through a freezing-out system 10 that reduced the water vapor pressure to 10^{-3} mm Hg. The gas temperature in chamber 6 was measured by a thermometer 5. As a spot check the speed of sound in the gas under investigation was measured with a sound interferometer 8 correct to $\pm 0.3\%$. The speed of the model was measured over two sections of the trajectory: in the auxiliary chamber (position 3) and after leaving the working chamber (position 7).

The speed was determined by measuring the time taken by the model to traverse a fixed distance. The block diagram of the equipment for measuring the speed is shown in Fig. 2. Type FEU-19M photomultipliers, operating in the light-partial shade regime, were used as sensors.

Two collimator systems, consisting of constant light sources 1 and condenser lenses 2, produce plane-parallel beams of light which intersect the trajectory at right angles. The objectives 3 focus the plane of the trajectory on slits 0.1 mm wide (4), through which the light falls onto the photocathodes of the photomultipliers 'a'. The moving object modulates the light beam, generating an electrical pulse whose shape depends on the model configuration. By way of example, Fig. 3 shows the pulses obtained as a result of intersection of the light beam by a sphere (oscillogram 'a') and a conical-cylindrical model (oscillogram 'b'). Since the amplitude of the photomultiplier signal is not enough to trigger the timer IV-13M, these signals are amplified and shaped. In order to eliminate errors due to a possible difference in amplification channel characteristics, a single-channel unit with pulse separation at the output was used (see Fig. 2). Signals from the cathode followers b are fed into a channel c where they are amplified, clipped to eliminate noise, and

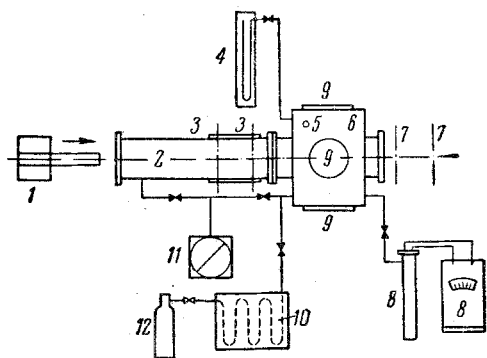


Fig. 1.

differentiated. The phase selector d discriminates either the leading or the trailing edge of the pulses. After amplification in unit e, the signals are fed to the output cathode followers f. The cathode follower connected to the second input of the IV-13M is biased off and in the normal position does not transmit the pulse from the first photomultiplier. The 400 μ sec switching pulse is produced by a univibrator g, triggered by the pulse from the first photomultiplier. The necessary switching pulse delay is ensured by an integrating circuit at the univibrator output. For a signal amplitude of 0.05-0.1 V at the photomultiplier load the output signal has an amplitude of up to 40 V with a front of 0.1 μ sec.

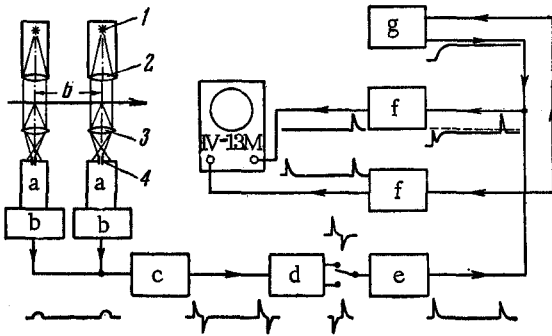


Fig. 2.

The essence of the method consists in the automatic photometric measurement of the flow spectrum and the model silhouette by means of photoelectronic attachments to the corresponding optical systems.

The Topler system 3 ensures visualization of the forward shock wave over a wide range of initial pressures in the working chamber. A DKSSh-1000 lamp was used as the light source 6. The silhouette optical system is mounted vertically. Only the outline of the model is reproduced in the image plane of the objective 4, since the light source 1 has a mat exit face, and, moreover, the light is additionally scattered by a mat screen 2. In the image planes of the two optical systems lie the slits of the photoelectronic attachments 9 and 5; these slits are 0.05 mm wide ($\sim 1/300$ of the diameter of the model image). Before the measurements are made, the slits are adjusted so that they are perpendicular to the trajectory and superimposed in the same plane.

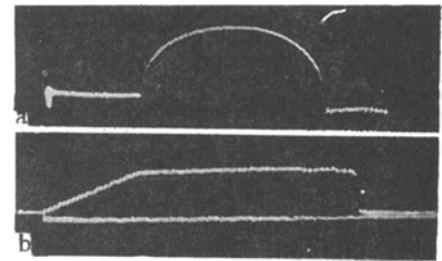


Fig. 3.

At the instant when the image of the flow spectrum and the model silhouette pass the slits, signals are generated at the photomultiplier loads; these are registered by a dual-trace DESO-1 oscilloscope; in the diagram, 10 is the oscilloscope, 11 and 12 are the first and second channels, 13 is the trigger. The detachment distance in the time expression τ (Fig. 4) can be measured as the time difference between the arrival of the leading edges of the pulses in the horizontal sweep of the oscilloscope. The linear detachment distance is $\Delta = \tau v$, where v is the model velocity.

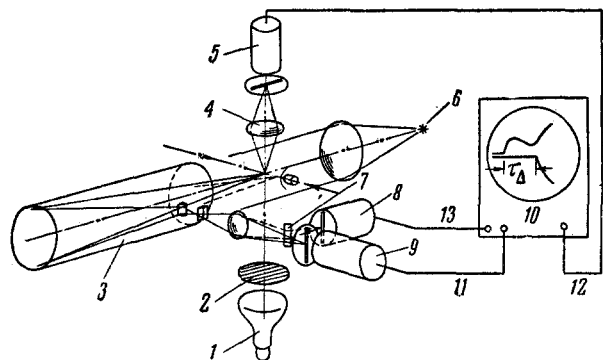


Fig. 4.

Preliminary superposition of the photomultiplier slits 9 and 5 was checked correct to a slit half-width in control experiments at subsonic speeds, with both photoelectronic attachments detecting only the outline of the model. The driven sweep of the oscilloscope was triggered by a signal from photomultiplier 8, whose slit is displaced slightly upwards with respect to the trajectory. The image of the flow spectrum falls on the slit of photomultiplier 8 after reflection from the mirror 7.

Figure 5 shows oscillograms obtained from photometric measurements of the flow spectra and silhouettes of

hemispherical models at different speeds. Oscillogram 'a' gives the entire flow picture, including the region of the base trace. The result of preliminary superposition of the photomultiplier slits can be clearly seen (the leading edges of the model pulses from both photomultipliers coincide). Oscillogram 'b' corresponds to a model moving at a velocity close to the speed of sound in the gas. Now the leading edges of the shock wave and the body can be fixed by a single photo-electronic attachment of the Topler system. Oscillogram 'c' reflects the result of measuring the flow spectrum and silhouette of the forward part of the model at $M > 3$. The time marks — length $2.5 \mu\text{sec}$ (oscillogram 'b') and $0.1 \mu\text{sec}$ (oscillogram 'c') — were supplied by a standard signal generator calibrated with a quartz heterodyne wavemeter.

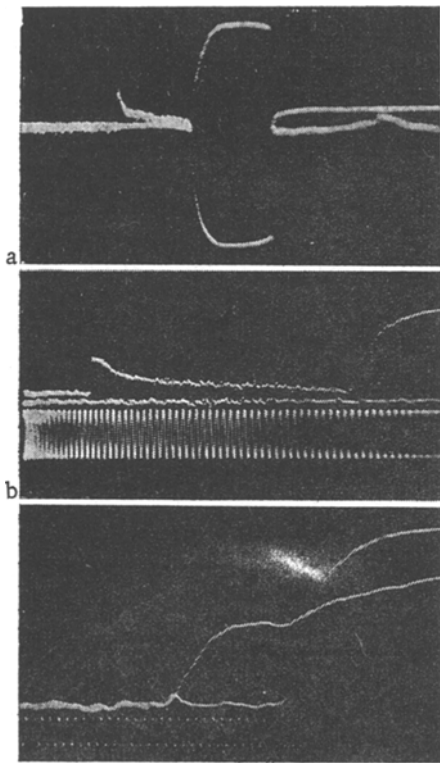


Fig. 5.

the experiments, the Reynolds number R — referred to the diameter of the model — was varied over the range 10^4 to 10^6 by changing the model dimensions, the flight speed, and the initial pressure in the working chamber. Within the range of M and R numbers in question, the flow in the shock layer may be considered essentially nonviscous [1, 7]. In all the experiments the initial temperature of the gas was constant and equal to 290°K .

The results of measurements of shock detachment from a hemispherical model 15 mm in diameter in air are shown in Fig. 6. The Mach number, M , is plotted along the axis of abscissas and the detachment distance Δ , relative to the radius of the hemisphere, along the axis of ordinates. The measurements were made at initial pressures $p = 100 \text{ mm Hg}$ (points 4) and $p = 1 \text{ atm}$ (points 3). Figure 6 also shows the results of theoretical calculations of flow past a hemisphere of a gas with a constant ratio of the specific heat capacities $\gamma = c_p/c_v = 1.4$ [8] (curve 1), and an equilibrium air flow for $p = 1 \text{ atm}$ and $T = 280^\circ\text{K}$ [9] (curve 2). At $M > 3$ the experimental values of Δ begin to depend on the initial pressure in the working chamber. The points corresponding to $p = 100 \text{ mm Hg}$ agree with the theoretical curve for $\gamma = 1.4 = \text{const}$ over the entire range of Mach numbers, but the points obtained for $p = 1 \text{ atm}$ lie below this curve, though still above the theoretical data for equilibrium flow.

Thus, under the experimental conditions for $p = 100 \text{ mm Hg}$ the vibrations of the air molecules in the shock layer are completely "frozen," while for $p = 1 \text{ atm}$ the excitation is nonequilibrium. For $M = 6$ in air, the gas temperature behind a normal shock — computed for equilibrium vibrational excitation — reaches 2000°K . This temperature corresponds to almost total excitation of the oxygen molecules (the characteristic excitation temperature for oxygen $\theta(\text{O}_2) = 2228^\circ\text{K}$) excitation of the nitrogen molecules $\theta(\text{N}_2) = 3336^\circ\text{K}$.

Moreover, since the vibrational relaxation time for oxygen over this temperature range is an order less than the

The total measuring error using this method does not exceed $\pm 5\%$. The accuracy can be increased by using a large-caliber model or by reducing the model speed.

Under conditions of supersonic free flight we measured the detachment for hemispherical models in air and carbon dioxide. The model speed was varied over the range 500 to 2100 m/sec. Using the known relation between the detachment distance and the degree of compression of the gas for a normal shock [1, 5, 6] we can estimate the excitation of internal degrees of freedom from the change in the quantity $K = \rho_2/\rho_1$. Such an estimate indicates that up to a velocity of $v = 2100 \text{ m/sec}$ in air and carbon dioxide it is essentially only vibrational degrees of freedom of the molecules that are excited. Under ballistic experiment conditions, real gas effects are most easily detected by varying the initial pressure in the working chamber for the same Mach number M .

Given equilibrium vibrational excitation the initial pressure will have no effect on the flow parameters, and hence on the detachment distance. In this case, a change of pressure will affect only the width of the relaxation zone.

In reducing the pressure in the working chamber, it is also necessary to take into account the possibility of the appearance of effects associated with interaction between the shock wave and the boundary layer. During

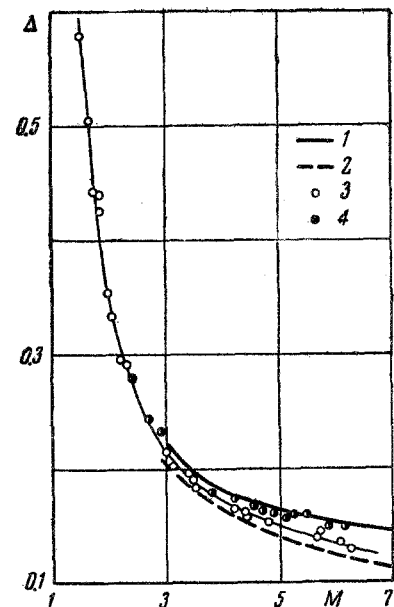


Fig. 6.

excitation time for nitrogen [10], it may be assumed that for $M \approx 6$ in air the vibrations in the oxygen molecules correspond to equilibrium excitation, while in the nitrogen they remain "frozen". A more accurate understanding of the kinetics of vibrational excitation of the molecules that enter into the composition of air can be obtained by comparing the experimental data with the results of calculations of the nonequilibrium flow of air past a hemisphere for the same initial conditions.

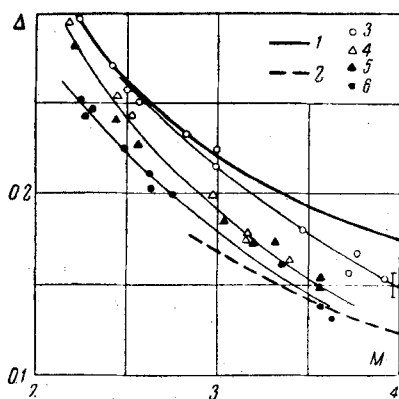


Fig. 7.

For the investigations in carbon dioxide, a hemispherical model 57 mm in diameter was used. Figure 7 shows the results for the dimensionless detachment distance over the range $M = 4$ for initial pressures $p = 10$ mm (points 3), $p = 50$ mm (points 4, 5), and $p = 1$ atm (points 6). It also gives the results of theoretical calculations of the flow past a hemisphere of a gas with $\gamma = 1.4 = \text{const}$ [8] (curve 1) and an equilibrium flow of carbon dioxide for $p = 1$ atm and $T = 280^\circ\text{K}$ [9] (curve 2).

Since over the range of shock wave intensities considered, the presence of water vapor [11] may affect the vibrational relaxation time in carbon dioxide, the experiments at $p = 50$ mm Hg were carried out in both dried (points 4) and undried gas (points 5). These measurements showed that the dryness of the carbon dioxide gas did not significantly affect the detachment distance. The experimental points lay on one curve, within the limits of accuracy of the measurements.

Variation of the initial pressure of the carbon dioxide for a fixed Mach number led to a significant change in the detachment distance, just as with air. At $p = 10$ mm Hg, up to $M = 3$ the measurements coincide with the calculated curve corresponding to total "freezing" of the vibrations ($\gamma = 1.4 = \text{const}$), although before the shock vibrations in the CO_2 are partially excited even at room temperature ($\gamma = 1.29$). The experimental points obtained for $p = 1$ atm lie close to the theoretical curve corresponding to equilibrium flow. Finally, at $p = 50$ mm Hg, the measurements lie between the "frozen" and the equilibrium theoretical curves.

At all values of the initial pressure, the change in detachment distance with increase in Mach number indicates a tendency for thermodynamic equilibrium to be established in the shock layer, and the experimental points corresponding to $p = 1$ atm and $M \approx 4$ coincided with the calculated data for equilibrium flow.

At present we have no clear ideas on the rate of excitation of the different vibrational degrees of freedom in CO_2 molecules, and the experimental data concerning the detachment distance may be useful in solving this problem.

Thus, by measuring the position of the detached shock in air and CO_2 with different initial experimental conditions, we investigated the change in detachment distance in relation to the various degrees of vibrational excitation of the molecules in the shock layer. The flow regimes corresponding to total "freezing" and to equilibrium and nonequilibrium vibrational excitations were observed.

REFERENCES

1. N. Schwartz and J. Eckerman, "Shock location in front of a sphere as a measure of real gas effect," *J. Appl. Phys.*, vol. 27, no. 2, p. 169, 1956.
2. G. Nagamatsu, R. Geiger, and R. Shir, "The influence of real gas effects on hypersonic flow past blunt bodies," *Vo pr. raketn. tekhn.*, Collection of translations and reviews of foreign literature, no. 11, 1960.
3. K. R. Lobb, "Hypersonic research at the Naval Ordnance Laboratory," *Proc. Eleventh Symposium of the Coloton Soc. held in University of Bristol, London, 1960.*
4. G. F. Telenin, "Gas flow in the presence of nonequilibrium physicochemical transitions," *Second All-Union Congress on Theoretical and Applied Mechanics; authors' summaries [in Russian], Moscow, p. 139, 1964.*
5. H. Serbin, "Supersonic flow around blunt bodies," *J. Aeronaut. Sci.*, vol. 25, no. 1, 1958.
6. A. Ambrosio and A. Wortman, "Stagnation-point shock-detachment distance for flow around spheres and cylinders in air," *J. Aerospace Sci.*, vol. 29, no. 7, 1962.
7. T. K. Herring, "The boundary layer near the stagnation point in hypersonic flow past a sphere," *J. Fl. Mech.*, vol. 7, part 2, 1960.
8. O. M. Belotserkovskii, "Calculation of flow around axisymmetric blunt bodies with a detached shock wave," [in Russian], *Izd. VTs AN SSSR, 1961.*
9. G. S. Roslyakov and G. F. Telenin, "Review of work on the calculation of steady-state axisymmetric gas flows at Moscow State University," *Collection: Numerical Methods in Gas Dynamics [in Russian], vol. II, Izd. MGU, 1963.*
10. J. L. Stollery and A. Smith, "Note on the variation of vibrational temperature along a nozzle," *J. Fl. Mech.*,

vol. 13, part 2, 1962.

11. E. F. Smiley and E. H. Winkler, "Shock-tube measurements of vibrational relaxation," J. Chem. Phys., vol. 22, no. 12, 1954.

8 June 1964

Leningrad